Energetic costs of calcification under ocean acidification

Christopher Spalding[1] [ID], Seth Finnegan[2], and Woodward W. Fischer[1]

[1]Division of Geological and Planetary Sciences, California Institute of Technology, Pasadena, California, USA, [2]Department of Integrative Biology, University of California, Berkeley, California, USA

Abstract Anthropogenic ocean acidification threatens to negatively impact marine organisms that precipitate calcium carbonate skeletons. Past geological events, such as the Permian-Triassic Mass Extinction, together with modern experiments generally support these concerns. However, the physiological costs of producing a calcium carbonate skeleton under different acidification scenarios remain poorly understood. Here we present an idealized mathematical model to quantify whole-skeleton costs, concluding that they rise only modestly (up to ~10%) under acidification expected for 2100. The modest magnitude of this effect reflects in part the low energetic cost of inorganic, calcium carbonate relative to the proteinaceous organic matrix component of skeletons. Our analysis does, however, point to an important kinetic constraint that depends on seawater carbonate chemistry, and we hypothesize that the impact of acidification is more likely to cause extinctions within groups where the timescale of larval development is tightly constrained. The cheapness of carbonate skeletons compared to organic materials also helps explain the widespread evolutionary convergence upon calcification within the metazoa.

Plain Language Summary Human activity continues to raise atmospheric levels of carbon dioxide, a gas that tends to increase the acidity of the world's oceans. Numerous marine species, such as corals and many types of shellfish, must manufacture skeletons of calcium carbonate, a mineral that is susceptible to corrosion in acidified seawater. This mineral is shaped into intricate and unique structures by way of an organic matrix that the organism must also generate. It remains poorly understood how much more energy organisms will need to expend in order to continue making their skeletons as ocean acidification continues. In this work, we use a simple mathematical approach to model the dependence of the calcification process to seawater chemistry. We find that the organic component of the skeleton is typically more costly than the calcium carbonate, mineral component. Therefore, the effect of acidification is somewhat damped in organisms possessing a more organic-rich skeleton. Owing to the relatively low sensitivity, we conclude that larval stages, when organisms are under much tighter constraints, are more critical for determining the impact of acidification upon a given group of organisms.

1. Introduction

Organisms that produce calcium carbonate ($CaCO_3$) skeletons are important members of the majority of marine ecosystems and comprise a substantial component of economic fisheries [*Waldbusser et al.*, 2013; *Ekstrom et al.*, 2015]. In addition, calcifying organisms are tightly coupled to the Earth's geological carbon cycle, with the global burial of carbonate-derived, biogenic carbon outweighing organic carbon [*Archer*, 2010]. Anthropogenic CO_2 input into the oceans is perturbing the carbonate chemistry of seawater [*Le Quéré et al.*, 2009], while geological feedbacks will take millennia to undo these effects [*Archer*, 2005; *Zachos et al.*, 2005]. In particular, the carbonate ion concentration ($[CO_3^{2-}]$) projected for year 2100 is about half preindustrial levels [*Orr et al.*, 2005; *Doney et al.*, 2009]. A critical outstanding problem is to understand how much more energy organisms may need to expend in future oceans if they are to maintain their biogenic rates of calcification, and how these additional costs may influence extinction risks.

Ancient events in the geological record evince the suspected influence of ocean acidification upon marine calcifiers [*Hönisch et al.*, 2012]. For example, the Permian-Triassic Mass Extinction, the greatest in the Phanerozoic, is notable for its strong selectivity against heavily calcified marine invertebrates. Its coincidence with carbon cycle perturbations suggests that elevated CO_2 levels and ocean acidification were to blame [*Knoll et al.*, 2007; *Knoll and Fischer*, 2011; *Payne and Clapham*, 2012]. Furthermore, differential extinction rates among

calcifiers contributed to a permanent, global shift from brachiopod to bivalve-dominated benthic assemblages [*Sepkoski*, 1981; *Bambach*, 1993; *Fraiser and Bottjer*, 2007; *Clapham and Bottjer*, 2007; *Liow et al.*, 2015; *Garbelli et al.*, 2016]. In contrast, other intervals of ocean acidification, such as during the Paleocene-Eocene Thermal Maximum, did not show a similarly strong selective extinction of marine calcifiers [*Zachos et al.*, 2005; *Thomas*, 2007; *McInerney and Wing*, 2011; *Knoll and Fischer*, 2011]. Accordingly, the fossil record implies a certain degree of coupling between ocean pH and the success of calcifying organisms, but the relationship is not straightforward and varies among taxa [*Ries et al.*, 2009].

In response to the modern acidification crisis, numerous laboratory and mesocosm experiments have sought to determine the differential susceptibility of calcifying taxa to ocean acidification [*Doney et al.*, 2009; *Hofmann et al.*, 2010; *Barton et al.*, 2012; *Gazeau et al.*, 2013]. In general, marine invertebrates exhibit decreased rates of calcification under more acidic conditions, but it has remained challenging to relate these results to species-wide extinction risks. Experiments have often focused upon adult individuals; however, the importance of larvae for dispersal [*Cowen and Sponaugle*, 2009] and their characteristically high mortality rates suggest that stresses upon larval stages may have a disproportionate influence on survivorship and extinction risk.

More recent investigations have increasingly focused on acidification stress experienced during early ontogenetic stages, the larvae and juveniles [*Albright et al.*, 2010; *Waldbusser et al.*, 2013, 2015a, 2015b, 2016; *Frieder et al.*, 2016; *Bylenga et al.*, 2017]. These earlier life stages experience two additional physiological constraints when compared to their adult forms. Specifically, the first shell, deposited during the larval stage in brachiopods and bivalves and during settlement in corals [*Kurihara*, 2008], must be manufactured within a sufficiently short period of time (1–2 days in bivalves and brachiopods); otherwise, the chances of surviving to reproductive maturity are greatly decreased. We refer to this constraint as a "kinetic" constraint, meaning that calcium carbonate must be deposited at a high enough rate to satisfy developmental demands [*Stricker and Reed*, 1985; *Waldbusser et al.*, 2013]. Taxa that brood their young exhibit a relatively extended larval stage and appear to experience correspondingly reduced sensitivity to ocean acidification [*Waldbusser et al.*, 2016].

In addition to kinetic/time constraints, larvae often must generate their first shells using a limited energy resource, derived from the mother [*Waldbusser et al.*, 2013]. Accordingly, if shells become more expensive under lower pH, the larval energy budget leads to a smaller mass of shell deposited (as measured in the Pacific oyster, *Crassostrea gigas*) [*Frieder et al.*, 2016]. Accordingly, even when larvae calcify rapidly enough to satisfy their kinetic constraints, shells in acidified waters may simply become too energetically expensive to manufacture.

From laboratory experiments, it is often difficult to distinguish between a loss of shell mass owing to higher costs (in terms of joules per gram), and a loss of shell mass due to reduced calcification rates. Our goal in this work was to develop a simple, generalized model of calcification that captures the interplay between energetic/cost constraints and kinetic/time constraints.

We benchmarked our results against growth data from bivalves and brachiopods [*Stricker and Reed*, 1985; *Waldbusser et al.*, 2013], in part owing to these groups' relevance to the Permian-Triassic Mass Extinction, along with the general prevalence of these taxa in the Phanerozoic fossil record. Furthermore, experimental work has directly measured the metabolic carbon content of larval oyster shells [*Waldbusser et al.*, 2013], which is a property directly linked to kinetic constraints in our model. Our derived costs agree well with values obtained experimentally [*Palmer*, 1992; *Waldbusser et al.*, 2013; *Frieder et al.*, 2016].

1.1. Importance of Seawater Chemistry

During past acidification events, much of the extinction variability across species has undoubtedly stemmed from a combination of factors in addition to changing seawater carbonate chemistry, such as temperature, hypercapnia, and/or anoxia [*Pörtner et al.*, 2005]. Consequently, it is challenging to isolate the influence of carbonate chemistry. As a first step, consider abiogenic precipitation, which proceeds if the saturation state

$$\Omega \equiv \frac{[CO_3^{2-}] \; [Ca^{2+}]}{\kappa_{sp}}, \tag{1}$$

defined for a given $CaCO_3$ polymorph with equilibrium constant κ_{sp}, is greater than unity. Despite Ω being a thermodynamic quantity, the rate R_{calc} of precipitation (or dissolution) is often well approximated using the constitutive relationship [*Morse et al.*, 2007]

$$R_{calc} = k\,(\Omega - 1)^n, \tag{2}$$

where n is the reaction order and k is a constant, encoding factors such as surface area and temperature.

Most waters inhabited by calcifying organisms possess $\Omega > 1$ (for aragonite and calcite), and so a naive interpretation of equation (2) above would be that $CaCO_3$ may be obtained with zero energetic input; indeed, free energy is released during the precipitation process. However, abiogenic precipitation rates are typically orders of magnitude slower than the cadence required by calcifying organisms. Accordingly, calcifying taxa must expend energy by way of enhancing R_{calc} such as to meet their kinetic demands.

Two avenues for rate enhancement may be inferred from equation (2). First, an important difference between biogenic and abiogenic $CaCO_3$ formation is that organisms typically produce an organic matrix of posttranslationally modified glycoproteins that effectively increase k in equation (2) [*Lowenstam and Weiner*, 1989; *Cusack and Freer*, 2008; *Olson et al.*, 2012; *Waldbusser et al.*, 2013, *Waldbusser et al.*, 2015a]. These matrices acts as "templates," commonly utilizing acidic amino acid residues [*Gotliv et al.*, 2003; *Addadi et al.*, 2006] and specific structures in order to control which phase of $CaCO_3$ is stabilized and guide the intricate mineralogical fabrics common within skeletons. In order to determine the impact of ocean acidification upon whole-skeleton costs, it is essential to factor in the costs associated with these organic components.

The second way to enhance R_{calc} is to imbibe seawater into a calcifying compartment, wherein Ω is biochemically elevated [*Adkins et al.*, 2003; *Weiner and Addadi*, 2011]; it is this process that we model in the next section. Solid $CaCO_3$ can exist in skeletons as multiple metastable polymorphs, each with distinct solubilities and kinetics [*Brečević and Nielsen*, 1989; *Addadi et al.*, 2006; *Morse et al.*, 2007; *Weiner and Addadi*, 2011]. At increased Ω, the least soluble polymorphs, such as calcite, become oversaturated before the more soluble phases, such as amorphous calcium carbonate (ACC); however, the more soluble ACC precipitates faster than calcite if both are oversaturated, owing to its disordered structural configuration [*Gebauer et al.*, 2008]. It is now well established experimentally [*Weiss et al.*, 2002; *Addadi et al.*, 2006; *Weiner et al.*, 2009; *Weiner and Addadi*, 2011; *Gal et al.*, 2014] that calcifiers often produce ACC as a precursor (though evidence is still lacking for its presence within larvae), before allowing it to revert to a lower energy morph, for example, calcite or aragonite, that then forms part of the skeleton. The widespread use of ACC implies that biogenic calcification generally favors rapid kinetics.

As might be expected from the differences between biogenic and abiogenic precipitation, calcification rates in organisms display a significantly more complicated dependence on seawater chemistry than that implied by equation (2). Indeed, larval calcifiers are often able to deposit shell in waters that are undersaturated, though at reduced rates, and with functional abnormalities that may impair their ability to survive to adulthood [*Waldbusser et al.*, 2015a; *Frieder et al.*, 2016]. A possible reason for this effect is not necessarily that precipitating calcium carbonate becomes much more difficult at $\Omega < 1$ but that the shell deposited may undergo corrosion [*Nienhuis et al.*, 2010]. Here we focus on costs relevant to precipitation and ignore the impact of dissolution, equivalent to an assumption that $\Omega > 1$ in ambient seawater, but acknowledge that heightened sensitivity may arise owing to dissolution effects in the event that ocean acidification is extreme.

2. Physiological Costs of a $CaCO_3$ Skeleton

Previous work has suggested that the inorganic, $CaCO_3$ portion of skeletons is metabolically less costly per gram than the organic part [*Palmer*, 1983, 1992] suggesting a selective advantage for the evolution of organic-poor skeletons. On the other hand, adopting an ecology that depends upon $CaCO_3$ production introduces an evolutionary sensitivity to secular changes in seawater acid-base chemistry. Here "sensitivity" is related to the relative costs of the inorganic and organic components. Specifically, a skeleton possessing a greater investment in inorganic material will exhibit increased whole-shell sensitivity from ocean acidification as a larger fraction of its entire energetic demand will increase. In our framework, we assume that the fraction of the skeleton composed of organic material (matrix) relative to inorganic material (mineral) is fixed under acidification; such an assumption allows us to directly evaluate and compare the inorganic and organic costs.
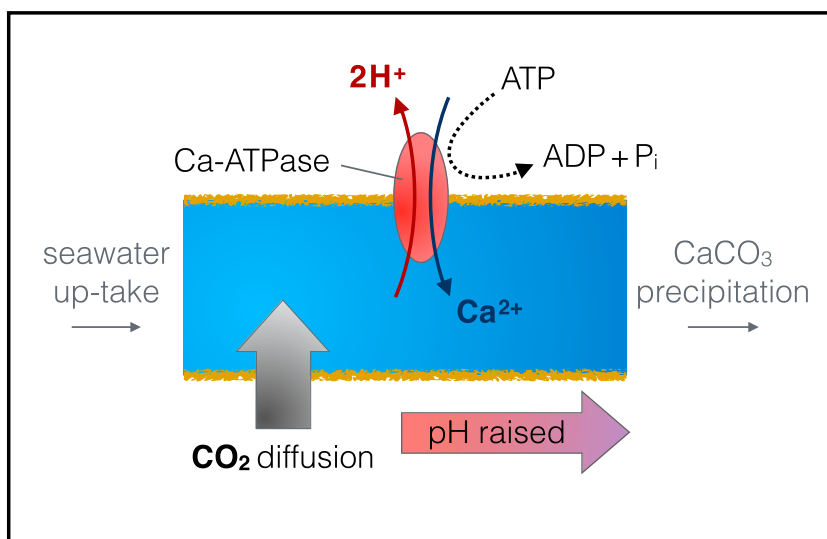
Figure 1. A schematic illustration of the calcification model. Seawater is taken into a calcifying space. Membrane-bound ATPase ion pumps introduce Ca^{2+} at the exchange of H^+ (with a ratio of 1:2), with the cost of ATP, in order to increase the carbonate concentration of the fluid and promote rapid calcification. CO_2 diffuses into the space from surrounding cells; this carbon is derived from respiration and has a distinct, ^{13}C-depleted, isotopic composition.

We constructed an idealized mathematical framework sufficiently general to model metabolic demand across a range of calcifying taxa, including extinct taxa that are otherwise beyond experimental investigation. Isotopic evidence suggests that the exact mechanisms of calcification are likely to vary significantly across taxa [*Adkins et al.*, 2003; *Cusack and Freer*, 2008] such that no model will ever capture the specific responses of all calcifiers in detail. However, nearly all marine calcifiers share a calcification pathway that involves the chemical alteration of seawater via ion pumping (Figure 1) in tandem with a diffusive flux of metabolically derived CO_2. The subsequent increase of Ω promotes rapid precipitation of $CaCO_3$, which is then guided into a specific structure using an organic matrix [*Lowenstam and Weiner*, 1989; *Zeebe and Sanyal*, 2002; *Adkins et al.*, 2003; *Erez*, 2003; *de Nooijer et al.*, 2009; *Bentov et al.*, 2009; *Vidavsky et al.*, 2014].

Costs associated with these key aspects of calcification are computed, alongside their dependence upon seawater chemistry. We identify observable consequences in the form of carbon isotopic signatures (resulting from the $\delta^{13}C$ signature of respired CO_2). The conclusions will be generalized, with each group of calcifying organisms exhibiting its own specific set of challenges in addition to those outlined here. The advantage of the general approach is to extract challenges that all calcifiers must face in order to produce carbonate phases from seawater at biologically meaningful rates.

Two end-member scenarios exist for the extraction of $CaCO_3$, which we term "batch" and "steady state" [*Gagnon et al.*, 2012]. Through the batch mechanism, a parcel of seawater is closed off and altered to the desired chemistry with little further seawater exchange. The final product, either highly supersaturated fluid or $CaCO_3$ itself, is then transported to the site of calcification. In the alternative, steady state picture the fluid chemistry is held relatively constant in time, where fluxes derived from precipitation, seawater mixing, metabolic CO_2 diffusion, and alkalinity pumping all balance each other [*Adkins et al.*, 2003]. At least in corals, isotopic analyses are consistent with either mechanism [*Gagnon et al.*, 2012], and both may operate in reality. Direct observations of batch-like calcification has been observed in foraminifera and cyanobacteria [*Erez*, 2003; *de Nooijer et al.*, 2009; *Bentov et al.*, 2009; *Benzerara et al.*, 2014].

Here we opted to focus our modeling on the batch process, but include a discussion of the steady mechanism in the supporting information. The steady state mechanism is conceptually similar to averaging over many parcels processed through the batch mechanism, meaning that the resulting behavior may be applied to both. From the point of view of calcification costs (Figure S3) a key difference between the models is that a steady state process can in principle yield $CaCO_3$ at zero cost to the organism (with an extreme example being to simply invoke supersaturated seawater as a starting point). However, as mentioned previously, such a strategy would produce skeletons at rates far too low to match the observed growth rates of calcifiers

[*Stricker and Reed*, 1985; *Waldbusser et al.*, 2013] and would not generate ACC, as is observed in most calcifying taxa. Therefore, we consider the costs of carbonate production at rates demanded by biological calcification and quantify how these might be reduced as a result of ocean acidification.

2.1. Model Description: Inorganic Component

In general, ATPase pumps are vital for cell acid-base balance [*Serrano*, 1989], of these, Ca-ATPase pumps are thought to dominate the calcification process [*Zeebe and Sanyal*, 2002; *Adkins et al.*, 2003; *Gagnon et al.*, 2012]. These ion pumps are membrane-bound, and calcifying spaces are adjacent to cells characterized by large concentrations of metabolically derived CO_2. Due to its nonpolar nature, this isotopically light CO_2 diffuses into the calcifying space, acting antagonistically to the effect of the pumps. Accordingly, in our calcification model, we begin with a membrane-bound parcel of seawater whose chemistry subsequently evolves by way of the removal of $2H^+$ ions for every Ca^{2+} ion introduced, together with an inward CO_2 flux from adjacent cells (Figure 1).

We assume that the CO_2 concentration of the calcifying fluid ($[CO_2]_{calc}$) is negligible compared to that of the cell, $[CO_2]_{cell}$. This assumption is valid for taxa lacking photosynthetic symbionts (or those with zooxanthellae but in the dark) but may become less exact otherwise [*Hohn and Merico*, 2012]. Consequently, the diffusive flux of dissolved inorganic carbon (DIC) into the fluid is approximately determined by the CO_2 concentration of the adjacent cell alone. In order to close the equations, we utilize the concept of Total Alkalinity ($[TA]$), which is the degree of acid titration required for a solution to reach a predefined fixed point [*Zeebe and Wolf-Gladrow*, 2001]. Pumping $2H^+$ out of the fluid increases $[TA]$ by two units. The fluid chemistry is therefore governed by the following equations [*Adkins et al.*, 2003]:

$$V\frac{d[TA]}{dt} = 2R_p$$
$$V\frac{d[DIC]}{dt} = \tilde{v} A \Delta [CO_2],$$
(3)

where V and A are the volume and surface area of the calcifying space, R_p is the molar rate of Ca^{2+} ion pumping, and $\tilde{v}$ is the (unknown) membrane permeability to CO_2 diffusion. Within the relevant pH range, a good approximation for carbonate concentration is [*Zeebe and Wolf-Gladrow*, 2001]

$$\left[CO_3^{2-}\right] \approx [TA] - [DIC].$$
(4)

There are several uncertain quantities in equation (3); $\tilde{v}$, V, and A, together with the pumping rate R_p, all constitute free parameters. We combine these parameters into characteristic quantities with the dimensions of time and flux, before scaling the variables in equation (3), removing dimensions from the problem. A natural timescale for the problem is the "residence time" of carbon in the calcifying fluid; i.e., the time $\mathcal{T}$ over which the incoming flux of metabolic carbon ($\mathcal{F} \equiv \tilde{v} A \Delta[CO_2]$) replaces the DIC originally obtained from seawater ($V[DIC]_{sw}$). Additionally, we remove dependence upon membrane permeability $\tilde{v}$ by parameterizing the ion pumping rate R_p as a fraction ϵ of $\mathcal{F}$. The problem is then scaled according to

$$\mathcal{F} = \tilde{v} A \Delta[CO_2]$$
$$R_p = \epsilon \mathcal{F}$$
$$\mathcal{T} = \frac{V[DIC]_{sw}}{\mathcal{F}},$$
(5)

leading to a simplified form for equation (3) (supporting information).

It is important to note that our scaled pumping parameter ϵ will change across taxa entirely owing to variations in CO_2 flux (for example, owing to hosting photosynthetic symbionts) even if their intrinsic pumping rates are the same. As we show below, however, ϵ is directly related to the metabolic carbon fraction. Accordingly, perhaps the strongest feature of the dimensionless model is that our results can be framed in terms of a measurable quantity — the metabolic fraction of carbon in the skeleton [*McConnaughey et al.*, 1997; *Adkins et al.*, 2003; *Gillikin et al.*, 2007; *Waldbusser et al.*, 2013].

The pumping of one Ca^{2+} ion costs an energy equivalent of one ATP molecule, the hydrolysis of which releases $\eta \approx 30$ kJ mol^{-1} [*Adkins et al.*, 2003]. Accordingly, the system of equation (3) yields the energy expenditure

and $[CO_3^{2-}]$ as a function of time. In order to calculate the mass-specific cost of calcification, we must decide upon a time $t' = t'_{end}$ at which the organism ceases pumping, together with how much calcium carbonate precipitates.

A reasonable end point to choose is when the fluid reaches a pH equal to $pK_2 (\approx 8.9$ in seawater), at which roughly half of the DIC is in the form of carbonate [*Zeebe and Wolf-Gladrow*, 2001]

$$\left[CO_3^{2-}\right]_{end} = \gamma[DIC]_{end}, \tag{6}$$

where $\gamma = 1/2$. This is consistent with typical pH ranges observed within organisms' calcifying spaces, including foraminifera [*de Nooijer et al.*, 2009] and corals [*McCulloch et al.*, 2012a]. In the interest of simplicity, we assume that all carbonate ions precipitate as solid $CaCO_3$, though in reality some fraction $(1-\alpha)$ will remain in solution. Accordingly, all of our derived costs should in principle be multiplied by α but the general conclusions will remain the same provided α is of order unity.

There is evidence that the surrounding seawater pH may influence the pH at which calcification occurs, with the relationship positive in corals [*McCulloch et al.*, 2012a, 2012b] but negative in benthic foraminifera [*Marchitto et al.*, 2014]. Accordingly, it is possible, in principle, that organisms may alter the end point of this process. As demonstrated in Figure S1, increasing γ from 0.5 to unity introduces a maximum increase in cost of about 40%, but the resulting calcification rate decreases (see equation (14) below), and it is unclear how tightly constrained this end point is. With that in mind, our derived sensitivities here may be regarded as upper limits, with phenotypic plasticity providing an uncertain degree of damping to the impact upon cost.

We can now compute the time at which the end point is reached. Specifically, the ordinary differential equation (3) may be combined, using relation (4), into a single differential equation for $[CO_3^{2-}]$ as a function of time. The chemistry of seawater comes into the problem as an initial condition upon $[CO_3^{2-}]$. All concentrations in the model are scaled by the DIC concentration of seawater, and so the initial condition is prescribed in terms of the fraction of seawater DIC in the form of bicarbonate:

$$x_2 \equiv \frac{\left[HCO_3^-\right]_{sw}}{[DIC]_{sw}}. \tag{7}$$

Solving the resultant equation for t'_{end} in terms of ϵ yields

$$t'_{end} = \frac{1 - 2x_2}{3 - 4\epsilon}. \tag{8}$$

It is important to emphasize that x_2 increases under short-term CO_2 input to the oceans (up to a maximum of unity); i.e., bicarbonate becomes more abundant at the expense of carbonate, and so it is the sensitivity of our results to x_2 that determines the impact of ocean acidification. Over timescales of $\sim$100 kyr, carbonate compensation will return x_2 to similar levels as before [*Zachos et al.*, 2005; *Archer*, 2005].

Given a time t'_{end} and the energy expended per mole of ATP, we compute the cost of $CaCO_3$ per unit mass as

$$C = \frac{\eta}{\mu_C} \epsilon \frac{2x_2 - 1}{2(\epsilon - 1) + x_2}, \tag{9}$$

where $\mu_C = 100$ g mol^{-1} is the molar mass of $CaCO_3$ and $\eta \approx 30$ kJ mol^{-1} (see above). From this, we see that *the faster an organism pumps (provided $\epsilon > 1$), the cheaper its skeleton becomes.* If $\epsilon < 1$, the alkalinity pumps are not working fast enough to balance the flux of metabolic carbon coming from surrounding tissues; therefore, $\epsilon > 1$ is a reasonable assumption. Optimization for cost thereby provides an impetus for organisms to modify the chemistry of the calcifying fluid as rapidly as possible.

Suppose that the organism is pumping very fast (as expected in larvae; see below), such that $\epsilon - 1 \gg x_2/2$, the energetic cost increases approximately linearly with x_2. Heuristically, this dependence arises because the difference between the initial x_2 and the end point $\gamma = 0.5$ will grow as acidification proceeds, a realization arising from our model that was not immediately obvious from experimental investigation into macroscopic energy budgets. An additional mechanistic insight is that organisms may in principle compensate for larger x_2 by enhancing the pumping rate ϵ. However, here we return to the crucial point that for many taxa, larvae may be pumping at or near physiological capacity owing to tight time constraints and high mortality rates. Accordingly, raising ϵ is not an option — costs increase (and rates decrease, discussed later).

For a constant value of ϵ, x_2 currently takes a numerical value of ~ 0.85 and so even a rise to 0.95 — a worst-case scenario — can increase costs by up to roughly 25%. As $\epsilon \to \infty$ (such that negligible influx of DIC occurs before reaching the end point) the cost $C \to (\eta/\mu_C)(x_2 - 1/2) \approx 0.1$ J mg^{-1}, approximately consistent with experimental data from larval oysters [*Waldbusser et al.*, 2013], though lower than that deduced in adult gastropods (~ 1–2 J mg^{-1} [*Palmer*, 1992]), suggesting lower ϵ.

2.2. Relative Cost of Organic Components

The total metabolic demand of skeletal construction includes a significant energetic investment in the synthesis of organic biomineral matrices [*Palmer*, 1983; *Lowenstam and Weiner*, 1989; *Palmer*, 1992; *Cusack and Freer*, 2008] that typically comprise up to about 5 wt % of the skeleton, though this organic fraction varies widely, both across and within taxa [*Palmer*, 1983; *Marin et al.*, 2007; *Tambutté et al.*, 2015].

The organic costs are not well known, but a value derived from experimental data in molluscs stands at $\nu \sim 30$ J mg^{-1} [*Palmer*, 1983, 1992], roughly 100 times our estimated minimum inorganic cost C. Fundamental amino acid synthesis appears to be cheaper, at ~ 3 J mg^{-1} [*Pace and Manahan*, 2006; *Pan et al.*, 2015], potentially reflecting the complex, highly organized nature of matrix glycoproteins [*Lowenstam and Weiner*, 1989; *Cusack and Freer*, 2008; *Olson et al.*, 2012]. Here we display results for the experimentally derived matrix cost of $\nu \sim 30$ J mg^{-1} but show in the supporting information that the results are similar for matrix costs more akin to amino acid production.

The total energetic cost $\mathcal{E}$ of a given mass of shell comprising an organic matrix of mass fraction f_p is

$$\mathcal{E}\left(x_2, f_p\right) = C\left(1 - f_p\right) + \nu f_p. \tag{10}$$

For ease of discussion, we define a function that measures the sensitivity of whole-shell cost to changes in seawater chemistry. This function is expressed as the fractional increase in $\mathcal{E}$ for a given increase Δx_2 of the parameter x_2:

$$S \equiv \frac{1}{\mathcal{E}} \frac{\partial \mathcal{E}}{\partial x_2} \Delta x_2. \tag{11}$$

It is important to note that in order to specifically examine how the inorganic costs of a skeleton vary with seawater carbonate chemistry, we assumed f_p to be independent of x_2, i.e., that the fraction of the final shell comprised of organic material remains unchanged under acidification. Previous authors have hypothesized that in contrast, calcifiers may manufacture additional organic material in order to enhance the calcification rate under acidification [*Waldbusser et al.*, 2015a]. If indeed organisms adopt this strategy, it may alleviate some of the acidification stress upon calcification rate outlined in this work — albeit at much higher whole-skeleton costs.

2.3. Metabolic Carbon Fraction

As alluded to above, the pumping parameter ϵ is difficult to directly measure and so we present our results in terms of the fraction of metabolically derived carbon f_M present within the precipitated CaCO$_3$. Numerous experiments have inferred f_M in real organisms, across multiple ontogenetic stages, by way of shell-δ^{13}C content [*McConnaughey et al.*, 1997; *Adkins et al.*, 2003; *Gillikin et al.*, 2007; *Waldbusser et al.*, 2013]. Within our model, f_M is computed from the quantity of light CO$_2$ that has diffused into the calcifying space by time t'_{end}. Using the solutions to equation (3), we find that

$$f_M(t') = \frac{t'}{1 + t'}. \tag{12}$$

Substituting $t' = t'_{end}$ yields the relationship

$$f_M|_{t'_{end}} = \frac{x_2 - 1/2}{2\left(\epsilon - 1\right) + x_2}, \tag{13}$$

which relates the pumping parameter ϵ to the metabolic fraction of carbon in the final shell. High ϵ translates to faster calcification rates, allowing less time for isotopically light carbon to enter the calcifying fluid. Accordingly, larger ϵ (faster pumping) leads to decreased f_M.
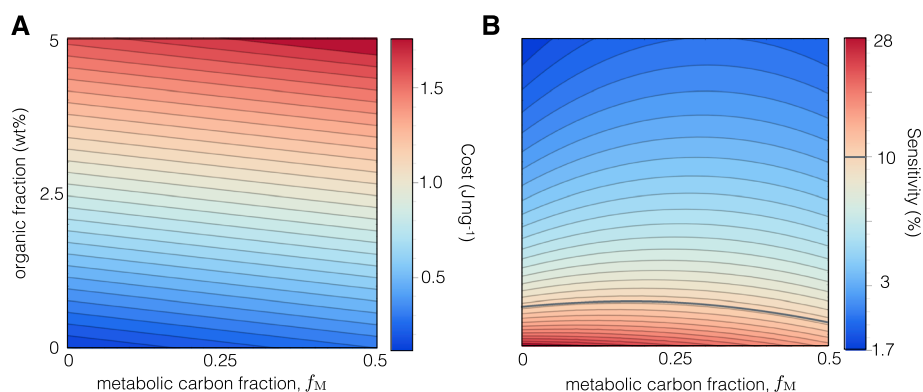
Figure 2. (a) Contours of skeletal costs per gram as a function of wt % organic material and metabolic carbon fraction (f_M). (b) Contours of calcification sensitivity S as a function of wt % organic material and f_M, assuming a change in seawater chemistry equivalent to $\Delta x_2 / x_2 = 0.1$ over the coming century. The thick grey line indicates a sensitivity of 10%. More active ion pumping translates to lower metabolic carbon fraction (leftward in the plots). Faster pumping always reduces the absolute cost but exhibits a nonmonotonic relationship to sensitivity. Higher organic fractions induce higher costs, but lower sensitivity (see discussion in text), suggesting an evolutionary trade-off between the two characters in individual lineages.

3. Results

With the above mathematical framework, we can compute the cost, in joules per gram, of a calcium carbonate skeleton as a function of the seawater carbonate chemistry statistic x_2 for a range of hypothetical skeleton compositions. In Figure 2, we present the cost and sensitivity S for a range of organic shell fractions f_p and metabolic carbon fractions f_M. Again, for this calculation we assume the inorganic and organic costs are independent and additive. We use $x_2 = 0.85$ [*Fabry et al.*, 2008; *Waldbusser et al.*, 2013] and $\Delta x_2 = 0.1$, within the range of recent the Intergovernmental Panel on Climate Change predictions for the next century [*Fabry et al.*, 2008; *Doney et al.*, 2009; *Comeau et al.*, 2013]. This is approximately equivalent to a 10% rise in x_2, though this value varies with geographic location.

Figure 2 illustrates that the greatest sensitivity to ocean acidification occurs at low organic fractions. This pattern may be understood by considering a shell containing no organic material at all ($f_p = 0$). In this case, acidification will increase the whole-shell cost by about 10–20% (from equation 9), roughly in line with limits obtained experimentally [*Gazeau et al.*, 2013]. However, if the more costly organic material is now incorporated, a relatively smaller fraction of the total shell cost is diverted to the manufacture of inorganic material, and so the proportional increase in skeletal cost under acidification is less than a purely inorganic skeleton would be. The color scale in Figure 2a is linear but logarithmic in Figure 2b, allowing the contours to illustrate that sensitivity to ocean acidification may be reduced by an order of magnitude by the incorporation of only a few per cent by mass organic material. In contrast, total cost increases by only a factor of 2–3.

These findings stem from the result that inorganic material costs on the order of 100 times less per gram than the organic matrix [*Palmer*, 1992]. Consequently, a hypothetical skeleton whose metabolic costs are equally partitioned between the inorganic and organic components will posses only a small wt % of organic material. In our model, we assumed that the organic fraction is not affected by changes in carbonate chemistry (x_2); however, *Tambutté et al.* [2015] demonstrated that the coral *Stylophora pistillata* produces a more organic-rich skeleton as pH is experimentally lowered. Quantitatively, the organic fraction increased by about 10% as pH was lowered from 7.95 to 7.2, or in the language of our model, the HCO_3^- fraction, x_2 rose from ~0.9 to ~0.94. Using our equation (9), this change in x_2 corresponds to roughly a 5–10% increase in inorganic costs, with this range spanning choices of ϵ from 1 all the way to infinity. Therefore, the observed change in organic fraction may naturally arise as a consequence of the coral setting aside a constant proportion of its metabolic investment to the inorganic and organic components across all pH values.

High values of ϵ reduce absolute cost but have a limited effect upon sensitivity, suggesting that fast pumping is in general beneficial, especially if lowering costs is paramount. This may explain in part why the rapid modification of the calcifying fluid and production of ACC appears to be a common strategy for calcifiers [*Gal et al.*, 2014].
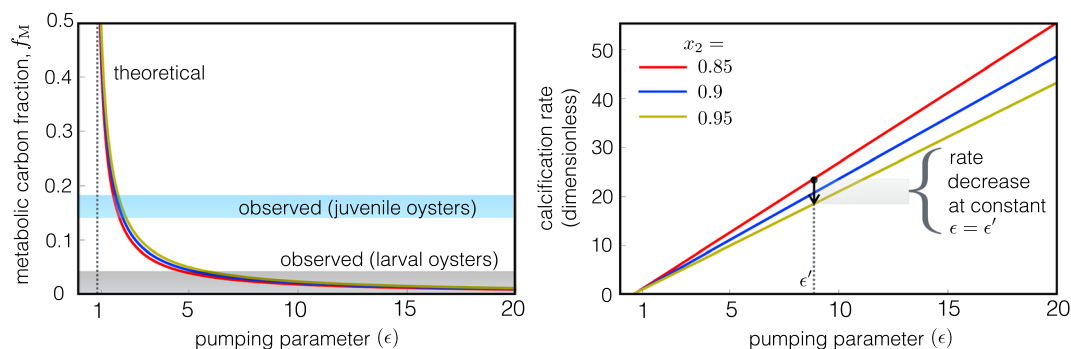
Figure 3. (left) The metabolic carbon fraction in the final $CaCO_3$ as a function of metabolic pumping effort during calcification. Lower f_M translates to shorter calcification times as less time is available for isotopically light carbon to diffuse in from neighboring tissues. (right) The influence of x_2 upon the calcification rate ($\mathcal{R}$) for a given value of ϵ. The low metabolic carbon values are typical for larval shells and suggest that they pump at or near physiological capacity. Acidification reduces this capacity, potentially impacting larval mortality.

Greater skeletal organic fractions reduce sensitivity to acidification, but crucially, this buffering effect does not apply to the *rate* at which calcification occurs (mass per time). We parametrize the rate as proportional to

$$\mathcal{R} \propto \frac{\gamma\left(1 + t'_{end}\right)}{t'_{end}} = \gamma \times \frac{1}{f_M}. \tag{14}$$

The above expression does not depend upon how much organic material is manufactured and added to the skeleton. Accordingly, a further insight of our model setup is that organic material buffers the sensitivity in cost, but not the rate, placing enhanced emphasis on the time constraints requisite to larval development, as opposed to their limited energy reserves.

A prediction of our model is that placing an organism within an environment that reduces its calcification rate should also lead to a rise in f_M. Unfortunately, as can be seen from Figure 3, the change in f_M occurring as a result of carbonate chemistry is small and may not be measurable. More importantly, however, for a given *physiologically determined* pumping efficiency ϵ', the effective calcification rate will decrease by about ~10% under acidification forecast for the coming century (Figure 3).

4. Potential Consequences of Ocean Acidification

Results from the calcification model highlight that energetic costs of inorganic $CaCO_3$ precipitation are increased by up to ~10–20% in response to a geologically brief input of CO_2 to the atmosphere and oceans, i.e., over a short timescale compared to that of carbonate compensation and silicate weathering feedbacks. However, when one considers that the organic component of the skeleton—despite its small relative mass—can cost as much or more than the inorganic fraction, the whole-skeleton cost increases more modestly (Figure 2). On the other hand, the maximum attainable calcification rate (Figure 3, right) is not subject to such buffering, lending kinetic limitations a particularly important role in survivorship, and therefore extinction risk.

Many marine organisms display their fastest mass-specific calcification rates while young. For example, the Pacific oyster (*Crassostrea gigas*) produces a shell equivalent to ~90% of its body mass within 2 days of fertilization [*Waldbusser et al.*, 2013], before allowing its mass-specific calcification rate to drop by an order of magnitude within 5 days (see Figure S4) [*Waldbusser et al.*, 2013]. A similar ontogenetic pattern has been observed in brachiopods [*Stricker and Reed*, 1985], implying that the earliest larval stages generally feel greater physiological pressure to calcify rapidly than juveniles and adults.

As a corollary of our model results, slower calcification rates correspond to heavier $\delta^{13}C$ signatures in skeletal carbonate. In Figure 3, we compare our model predictions relating f_M and ϵ to the measured f_M for larval ($f_M \sim 0.05$) and juvenile oysters ($f_M \sim 0.15$ [*Waldbusser et al.*, 2013]), with adults occupying a large range below about $f_M < 0.5$ [*Gillikin et al.*, 2007]. These ontogenic patterns suggest that the physiology of larvae have been evolutionarily sculpted for rapid calcification rates. In general, the observed fraction of metabolic carbon

increases throughout ontogeny across multiple species [*Gillikin et al.*, 2007]. Some changes in f_M are undoubtedly related to factors altering the CO_2 content of cells; however, our results suggest that the trend is *largely a manifestation of greater kinetic constraints during larval stages.*

If larvae calcify at or near their physiological limit, the effect of acidification will be to reduce the fraction of individuals that are capable of precipitating their initial skeleton sufficiently fast to reach the juvenile stages (Figure 3). Along this line of reasoning, evidence exists that bivalve larvae that undergo brooding, as opposed to broadcast spawning, exhibit reduced sensitivity to ocean acidification. Brooding lends more time to early shell development, hinting that larvae of these groups are not generally pumping at physiological capacity [*Waldbusser et al.*, 2016]. Consequently, these taxa may be able to increase ϵ to a degree, in response to acidification.

In contrast to the point of view of time constraints, larvae of *Crassostrea gigas* manufacture their earliest shell using energy mostly derived from their embryonic yolk [*Waldbusser et al.*, 2013], reducing their potential to compensate for higher calcification costs through feeding, even if they can meet a sufficient rate. It has been demonstrated that feeding during early ontogenetic stages can partly offset acidification stresses [*Edmunds*, 2011; *Drenkard et al.*, 2013]. Such tight constraints, both in terms of time and absolute energetic demand, during early life stages suggest that even the modest increases in calcification costs predicted by our model have the potential to substantially impact upon larval survival.

Numerous experimental efforts have pointed to the importance of ocean acidification on early life stages of calcifying taxa. For example, settlement in the reef coral *Porites* is significantly reduced under acidification forecast for the upcoming century [*Albright et al.*, 2010]. Furthermore, even in larvae not exhibiting acute acidification stress, such as the brooding oyster *Ostrea lurida*, later life stages display negative carryover effects which impact upon reproductive success [*Hettinger et al.*, 2012; *Waldbusser et al.*, 2016]. Cumulatively, we emphasize that larval survivorship may be the most crucial factor in determining which taxa are the most affected by acidification, and there is need of more experimentation examining the sensitivities of feeding versus nonfeeding taxa, as well as organisms with differing demands of early shell deposition (i.e., kinetic constraints).

4.1. Long-term Macroevolutionary Trends

The relatively low energetic cost associated with $CaCO_3$ compared to organic material helps explain why calcification has evolved many times independently in Earth history [*Knoll and Carroll*, 1999; *Marshall*, 2006; *Peters and Gaines*, 2012]: it is a cheap construction material for marine organisms. A consequence of this finding is that the independent acquisition of calcification across multiple metazoan lineages during the Cambrian Explosion and Ordovician Radiation [*Knoll and Carroll*, 1999; *Marshall*, 2006; *Peters and Gaines*, 2012] was unlikely to have been driven by a reduction in the cost of $CaCO_3$-precipitation stemming from high Ca concentrations [*Peters and Gaines*, 2012; *Kazmierczak et al.*, 2013]. Rather, our analysis here suggests that the cost-efficient precipitation of $CaCO_3$ requires only that a physiology facilitate a pumping parameter $\epsilon > 1$; membrane-bound Ca-ATPase pumps must be able to pump protons out of the calcifying fluid more rapidly than CO_2 diffuses across the membrane.

Despite its low cost, the adoption of a calcifying lifestyle introduces seawater carbonate chemistry as an additional constraint upon fitness. Our results show that such sensitivity to seawater saturation state may be damped through utilization of a more organic-rich skeleton, which is more costly, but less sensitive to seawater perturbations. Indeed, there is evidence that during the Permian-Triassic Mass Extinction, despite the Brachiopoda as a whole suffering a high extinction rate, brachiopod genera with more organic-rich skeletons preferentially survived [*Garbelli et al.*, 2016].

In contrast to the geologically brief Permian-Triassic Mass Extinction, there exists no apparent long-term trend toward more organic-rich skeletons over the Phanerozoic. Indeed, at least within the bivalves, there is some suggestion of the opposite trend [*Taylor*, 1973; *Marin et al.*, 2007]. Therefore, we conclude by noting that the global marine biota have, over evolutionary time achieved an approximate equilibrium between the high cost of an organic matrix, and the increased resistance to acidification that such a matrix offers. Shorter-term acidification events have demonstrated their potential to irreversibly disrupt this equilibrium. Considering the rapidity of the modern crisis, we suggest a greater experimental focus upon measuring the organic component of calcifier skeletons, alongside investigations into the sensitivity to acidification during early life stages, when the first shell is being formed.

References

Addadi, L., D. Joester, F. Nudelman, and S. Weiner (2006), Mollusk shell formation: A source of new concepts for understanding biomineralization processes, *Chem. Eur. J.*, *12*(4), 980–987.

Adkins, J. F., E. A. Boyle, W. B. Curry, and A. Lutringer (2003), Stable isotopes in deep-sea corals and a new mechanism for "vital effects", *Geochim. Cosmochim. Acta*, *67*(6), 1129–1143.

Albright, R., B. Mason, M. Miller, and C Langdon (2010), Ocean acidification compromises recruitment success of the threatened Caribbean coral Acropora palmata, *Proc. Natl. Acad. Sci. U.S.A.*, *107*(47), 20,400–20,404.

Archer, D. (2005), Fate of fossil fuel CO_2 in geologic time, *J. Geophys. Res.*, *110*, C09S05, doi:10.1029/2004JC002625.

Archer, D. (2010), *The Global Carbon Cycle*, Princeton Univ. Press, Princeton, N. J.

Bambach, R. K. (1993), Seafood through time: Changes in biomass, energetics, and productivity in the marine ecosystem, *Paleobiology*, *19*, 372–397.

Barton, A., B. Hales, G. G. Waldbusser, C. Langdon, and R. A. Feely (2012), The Pacific oyster, Crassostrea gigas, shows negative correlation to naturally elevated carbon dioxide levels: Implications for near-term ocean acidification effects, *Limnol. Oceanogr.*, *57*(3), 698–710.

Bentov, S., C. Brownlee, and J. Erez (2009), The role of seawater endocytosis in the biomineralization process in calcareous foraminifera, *Proc. Natl. Acad. Sci. U.S.A.*, *106*(51), 21,500–21,504.

Benzerara, K., et al. (2014), Intracellular Ca-carbonate biomineralization is widespread in cyanobacteria, *Proc. Natl. Acad. Sci. U.S.A.*, *111*(30), 10,933–10,938.

Brečević, L., and A. E. Nielsen (1989), Solubility of amorphous calcium carbonate, *J. Cryst. Growth*, *98*(3), 504–510.

Bylenga, C. H., V. J. Cummings, and K. G. Ryan (2017), High resolution microscopy reveals significant impacts of ocean acidification and warming on larval shell development in Laternula elliptica, *PLoS One*, *12*(4), e0175706.

Clapham, M. E., and D. J. Bottjer (2007), Permian marine paleoecology and its implications for large-scale decoupling of brachiopod and bivalve abundance and diversity during the Lopingian (Late Permian), *Palaeogeogr. Palaeoclimatol. Palaeoecol.*, *249*(3), 283–301.

Comeau, S., R. C. Carpenter, and P. J. Edmunds (2013), Coral reef calcifiers buffer their response to ocean acidification using both bicarbonate and carbonate, *Proc. R. Soc. B*, *280*(1753), 20122374.

Cowen, R. K., and S. Sponaugle (2009), Larval dispersal and marine population connectivity, *Annu. Rev. Mar. Sci.*, *1*, 443–466.

Cusack, M., and A. Freer (2008), Biomineralization: Elemental and organic influence in carbonate systems, *Chem. Rev.*, *108*(11), 4433–4454.

de Nooijer, L. J., T. Toyofuku, and H Kitazato (2009), Foraminifera promote calcification by elevating their intracellular pH, *Proc. Natl. Acad. Sci. U.S.A.*, *106*(36), 15,374–15,378.

Doney, S. C., V. J. Fabry, R. A. Feely, and J. A. Kleypas (2009), Ocean acidification: The other CO_2 problem, *Annu. Rev. Mar. Sci.*, *1*, 69–192.

Drenkard, E. J., A. L. Cohen, D. C. McCorkle, S. J. de Putron, V. R. Starczak, and A. E. Zicht (2013), Calcification by juvenile corals under heterotrophy and elevated CO_2, *Coral Reefs*, *32*(3), 727–735.

Edmunds, P. J. (2011), Zooplanktivory ameliorates the effects of ocean acidification on the reef coral Porites spp, *Limnol. Oceanogr.*, *56*(6), 2402–2410.

Ekstrom, J. A., et al. (2015), Vulnerability and adaptation of US shellfisheries to ocean acidification, *Nat. Clim. Change*, *5*(3), 207–214.

Erez, J. (2003), The source of ions for biomineralization in foraminifera and their implications for paleoceanographic proxies, *Rev. Mineral. Geochem.*, *54*(1), 115–149.

Fabry, V. J., B. A. Seibel, R. A. Feely, and J. C. Orr (2008), Impacts of ocean acidification on marine fauna and ecosystem processes, *ICES J. Mar. Sci.*, *65*(3), 414–432.

Fraiser, M. L., and D. J. Bottjer (2007), When bivalves took over the world, *Paleobiology*, *33*(3), 397–413.

Frieder, C. A., S. L. Applebaum, T.-C. F. Pan, D. Hedgecock, and D. T. Manahan (2016), Metabolic cost of calcification in bivalve larvae under experimental ocean acidification, *ICES J. Mar. Sci.*, doi:10.1093/icesjms/fsw213.

Gagnon, A. C., J. F. Adkins, and J. Erez (2012), Seawater transport during coral biomineralization, *Earth Planet. Sci. Lett.*, *329*, 150–161.

Gal, A., K. Kahil, N. Vidavsky, R. T. DeVol, P. U. Gilbert, P. Fratzl, and S. Weiner (2014), Particle accretion mechanism underlies biological crystal growth from an amorphous precursor phase, *Adv. Funct. Mater.*, *24*(34), 5420–5426.

Garbelli, C., L. Angiolini, and S. Z. Shen (2016), Biomineralization and global change: A new perspective for understanding the end-Permian extinction, *Geology*, *45*, 19–22, doi:10.1130/G38430.1.

Gazeau, F., L. M. Parker, S. Comeau, J. P. Gattuso, W. A. O'Connor, S. Martin, H.-O. Pörtner, and P. M. Ross (2013), Impacts of ocean acidification on marine shelled molluscs, *Mar. Biol.*, *160*(8), 2207–2245.

Gebauer, D., A. Völkel, and H. Cölfen (2008), Stable prenucleation calcium carbonate clusters, *Science*, *322*(5909), 1819–1822.

Gillikin, D. P., A. Lorrain, L. Meng, and F. Dehairs (2007), A large metabolic carbon contribution to the $\delta^{13}C$ record in marine aragonitic bivalve shells, *Geochim. Cosmochim. Acta*, *71*(12), 2936–2946.

Gotliv, B. A., L. Addadi, and S. Weiner (2003), Mollusk shell acidic proteins: In search of individual functions, *ChemBioChem*, *4*(6), 522–529.

Hettinger, A., E. Sanford, T. M. Hill, A. D. Russell, K. N. Sato, J. Hoey, M. Forsch, H. N. Page, and B. Gaylord (2012), Persistent carry-over effects of planktonic exposure to ocean acidification in the Olympia oyster, *Ecology*, *93*(12), 2758–2768.

Hofmann, G. E., J. P. Barry, P. J. Edmunds, R. D. Gates, D. A. Hutchins, T. Klinger, and M. A. Sewell (2010), The effect of ocean acidification on calcifying organisms in marine ecosystems: An organism-to-ecosystem perspective, *Annu. Rev. Ecol. Evol. Syst.*, *41*, 127–147.

Hohn, S., and A Merico (2012), Modelling coral polyp calcification in relation to ocean acidification, *Biogeosciences*, *9*(11), 4441–4454.

Hönisch, B., et al. (2012), The geological record of ocean acidification, *Science*, *335*(6072), 1058–1063.

Kazmierczak, J., S. Kempe, and B. Kremer (2013), Calcium in the early evolution of living systems: A biohistorical approach, *Curr. Org. Chem.*, *17*(16), 1738–1750.

Knoll, A. H., and S. B. Carroll (1999), Early animal evolution: Emerging views from comparative biology and geology, *Science*, *284*(5423), 2129–2137.

Knoll, A. H., R. K. Bambach, J. L. Payne, S. Pruss, and W. W. Fischer (2007), Paleophysiology and end-Permian mass extinction, *Earth Planet. Sci. Lett.*, *256*(3), 295–313.

Knoll, A. H., and W. W. Fischer (2011), Skeletons and ocean chemistry: The long view, in *Ocean Acidification*, edited by J. P. Gattuso and L. Hansson, pp. 67–82, Oxford Univ. Press, Oxford, U. K.

Kurihara, H. (2008), Effects of CO_2-driven ocean acidification on the early developmental stages of invertebrates, *Mar. Ecol. Prog. Ser.*, *373*, 275–284.

Le Quéré, C., et al. (2009), Trends in the sources and sinks of carbon dioxide, *Nat. Geosci.*, *2*(12), 831–836.

Liow, L. H., T. Reitan, and P. G. Harnik (2015), Ecological interactions on macroevolutionary time scales: Clams and brachiopods are more than ships that pass in the night, *Ecol. Lett.*, *18*(10), 1030–1039.

Lowenstam, H. A., and S. Weiner (1989), *On Biomineralization*, Oxford Univ. Press, New York.

Marchitto, T. M., W. B. Curry, J. Lynch-Stieglitz, S. P. Bryan, K. M. Cobb, and D. C. Lund (2014), Improved oxygen isotope temperature calibrations for cosmopolitan benthic foraminifera, *Geochim. Cosmochim. Acta*, *130*, 1–11.

Marin, F., G. Luquet, B. Marie, and D. Medakovic (2007), Molluscan shell proteins: Primary structure, origin, and evolution, *Curr. Top. Dev. Biol.*, *80*, 209–276.

Marshall, C. R. (2006), Explaining the Cambrian "explosion" of animals, *Annu. Rev. Earth Planet. Sci.*, *34*, 355–384.

McConnaughey, T. A., J. Burdett, J. F. Whelan, and C. K. Paull (1997), Carbon isotopes in biological carbonates: Respiration and photosynthesis, *Geochim. Cosmochim. Acta*, *61*(3), 611–622.

McCulloch, M., J. Falter, J. Trotter, and P. Montagna (2012a), Coral resilience to ocean acidification and global warming through pH up-regulation, *Nat. Clim. Change*, *2*(8), 623–627.

McCulloch, M., et al. (2012b), Resilience of cold-water scleractinian corals to ocean acidification: Boron isotopic systematics of pH and saturation state up-regulation, *Geochim. Cosmochim. Acta*, *87*, 21–34.

McInerney, F. A., and S. L. Wing (2011), The Paleocene-Eocene thermal maximum: A perturbation of carbon cycle, climate, and biosphere with implications for the future, *Annu. Rev. Earth Planet. Sci.*, *39*, 489–516.

Morse, J. W., R. S. Arvidson, and A. Lüttge (2007), Calcium carbonate formation and dissolution, *Chem. Rev.*, *107*(2), 342–381.

Nienhuis, S., A. R. Palmer, and C. D. Harley (2010), Elevated CO_2 affects shell dissolution rate but not calcification rate in a marine snail, *Proc. R. Soc. B*, *277*(1693), 2553–2558.

Olson, I. C., R. Kozdon, J. W. Valley, and P. U. Gilbert (2012), Mollusk shell nacre ultrastructure correlates with environmental temperature and pressure, *J. Am. Chem. Soc.*, *134*(17), 7351–7358.

Orr, J. C., et al. (2005), Anthropogenic ocean acidification over the twenty-first century and its impact on calcifying organisms, *Nature*, *437*(7059), 681–686.

Pace, D. A., and D. T. Manahan (2006), Fixed metabolic costs for highly variable rates of protein synthesis in sea urchin embryos and larvae, *J. Exp. Biol.*, *209*(1), 158–170.

Palmer, A. R. (1983), Relative cost of producing skeletal organic matrix versus calcification: Evidence from marine gastropods, *Mar. Biol.*, *3*, 287–92.

Palmer, A. R. (1992), Calcification in marine molluscs: How costly is it?, *Proc. Natl. Acad. Sci. U.S.A.*, *89*(4), 1379–1382.

Pan, T. C. F., S. L. Applebaum, and D. T. Manahan (2015), Experimental ocean acidification alters the allocation of metabolic energy, *Proc. Natl. Acad. Sci. U.S.A.*, *112*(15), 4696–4701.

Payne, J. L., and M. E. Clapham (2012), End-Permian mass extinction in the oceans: An ancient analog for the twenty-first century?, *Annu. Rev. Earth Planet. Sci.*, *40*, 89–111.

Peters, S. E., and R. R. Gaines (2012), Formation of the "Great Unconformity" as a trigger for the Cambrian explosion, *Nature*, *484*(7394), 363–366.

Pörtner, H. O., M. Langenbuch, and B. Michaelidis (2005), Synergistic effects of temperature extremes, hypoxia, and increases in CO_2 on marine animals: From Earth history to global change, *J. Geophys. Res.*, *110*, C09S10, doi:10.1029/2004JC002561.

Ries, J. B., A. L. Cohen, and D. C. McCorkle (2009), Marine calcifiers exhibit mixed responses to CO_2-induced ocean acidification, *Geology*, *37*(12), 1131–1134.

Sepkoski, J. J., Jr. (1981), A factor analytic description of the phanerozoic marine fossil record, *Paleobiology*, *7*(1), 36–53.

Serrano, R. (1989), Structure and function of plasma membrane ATPase, *Annu. Rev. Plant Biol.*, *40*(1), 61–94.

Stricker, S. A., and C. G. Reed (1985), The protegulum and juvenile shell of a Recent articulate brachiopod: Patterns of growth and chemical composition, *Lethaia*, *18*(4), 295–303.

Tambutté, E., A. A. Venn, M. Holcomb, N. Segonds, N. Techer, D. Zoccola, D. Allemand, and S. Tambutté (2015), Morphological plasticity of the coral skeleton under CO_2-driven seawater acidification, *Nat. Commun.*, *6*, 7368.

Taylor, J. D. (1973), The structural evolution of the bivalve shell, *Palaeontology*, *16*(3), 519–534.

Thomas, E. (2007), Cenozoic mass extinctions in the deep sea: What perturbs the largest habitat on Earth?, *Geol. Soc. Am. Spec. Pap.*, *424*, 1–23.

Vidavsky, N., S. Addadi, J. Mahamid, E. Shimoni, D. Ben-Ezra, M. Shpigel, S. Weiner, and L. Addadi (2014), Initial stages of calcium uptake and mineral deposition in sea urchin embryos, *Proc. Natl. Acad. Sci. U.S.A.*, *111*(1), 39–44.

Waldbusser, G. G., E. L. Brunner, B. A. Haley, B. Hales, C. J. Langdon, and F. G. Prahl (2013), A developmental and energetic basis linking larval oyster shell formation to acidification sensitivity, *Geophys. Res. Lett.*, *40*, 2171–2176, doi:10.1002/grl.50449.

Waldbusser, G. G., B. Hales, C. J. Langdon, B. A. Haley, P. Schrader, E. L. Brunner, M. W. Gray, and C. A. Miller (2015a), Saturation-state sensitivity of marine bivalve larvae to ocean acidification, *Nat. Clim. Change*, *5*(3), 273–280.

Waldbusser, G. G., B. Hales, C. J. Langdon, B. A. Haley, P. Schrader, E. L. Brunner, M. W. Gray, C. A. Miller, I. Gimenez, and G. Hutchinson (2015b), Ocean acidification has multiple modes of action on bivalve larvae, *PLoS One*, *10*(6), e0128376.

Waldbusser, G. G., M. W. Gray, B. Hales, C. J. Langdon, B. A. Haley, I. Gimenez, S. R. Smith, E. L. Brunner, and G. Hutchinson (2016), Slow shell building, a possible trait for resistance to the effects of acute ocean acidification, *Limnol. Oceanogr.*, *61*(6), 1969–1983.

Weiner, S., J. Mahamid, Y. Politi, Y. Ma, and L. Addadi (2009), Overview of the amorphous precursor phase strategy in biomineralization, *Front. Mater. Sci. Chin.*, *3*(2), 104–108.

Weiner, S., and L. Addadi (2011), Crystallization pathways in biomineralization, *Annu. Rev. Mater. Res.*, *41*, 21–40.

Weiss, I. M., N. Tuross, L. Addadi, and S. Weiner (2002), Mollusc larval shell formation: Amorphous calcium carbonate is a precursor phase for aragonite, *J. Exp. Zool.*, *293*(5), 478–491.

Zachos, J. C., et al. (2005), Rapid acidification of the ocean during the Paleocene-Eocene thermal maximum, *Science*, *308*(5728), 1611–1615.

Zeebe, R. E., and D. Wolf-Gladrow (2001), *CO_2 in Seawater: Equilibrium, Kinetics, Isotopes: Equilibrium, Kinetics, Isotopes*, Elsevier, Chicago, Ill.

Zeebe, R. E., and A. Sanyal (2002), Comparison of two potential strategies of planktonic foraminifera for house building: Mg^{2+} or H^+ removal?, *Geochim. Cosmochim. Acta*, *66*(7), 1159–1169.